Genetic variation of DNA methyltransferase-3A contributes to protection against persistent MRSA bacteremia in patients

Felix Mba Medie[a], Batu K. Sharma-Kuinkel[a], Felicia Ruffin[a], Liana C. Chan[b,c], Maura Rossetti[d], Yu-Ling Chang[d], Lawrence P. Park[a,e], Arnold S. Bayer[f,g,h], Scott G. Filler[f,g,h], Richard Ahn[d,h,i], Elaine F. Reed[d], David Gjertson[d,1], Michael R. Yeaman[b,f,g,1], Vance G. Fowler Jr.[a,j,1,2], and the MRSA Systems Immunobiology Group[3]

[a]Division of Infectious Diseases, Department of Medicine, Duke University School of Medicine, Durham, NC 27710; [b]Division of Molecular Medicine, Harbor–University of California, Los Angeles Medical Center, Torrance, CA 90502; [c]Los Angeles Biomedical Research Institute at Harbor–University of California, Los Angeles Medical Center, Torrance, CA 90502; [d]Department of Pathology and Laboratory Medicine, University of California, Los Angeles Immunogenetics Center, Los Angeles, CA 90095; [e]Duke Global Health Institute, Duke University, Durham, NC 27710; [f]Division of Infectious Diseases, Harbor–University of California, Los Angeles Medical Center, Torrance, CA 90502; [g]Department of Medicine, David Geffen School of Medicine, University of California, Los Angeles, CA 90095; [h]Department of Microbiology, Immunology, and Molecular Genetics, University of California, Los Angeles, CA 90095; [i]Institute for Quantitative and Computational Biosciences, University of California, Los Angeles, CA 90095; and [j]Duke Clinical Research Institute, Durham, NC 27705

Edited by Lawrence Steinman, Stanford University School of Medicine, Stanford, CA, and approved August 20, 2019 (received for review June 7, 2019)

The role of the host in development of persistent methicillin-resistant *Staphylococcus aureus* (MRSA) bacteremia is not well understood. A cohort of prospectively enrolled patients with persistent methicillin-resistant *S. aureus* bacteremia (PB) and resolving methicillin-resistant *S. aureus* bacteremia (RB) matched by sex, age, race, hemodialysis status, diabetes mellitus, and presence of implantable medical device was studied to gain insights into this question. One heterozygous g.25498283A > C polymorphism located in the *DNMT3A* intronic region of chromosome 2p with no impact in messenger RNA (mRNA) expression was more common in RB (21 of 34, 61.8%) than PB (3 of 34, 8.8%) patients ($P = 7.8 \times 10^{-6}$). Patients with MRSA bacteremia and g.25498283A > C genotype exhibited significantly higher levels of methylation in gene-regulatory CpG island regions (Δmethylation = 4.1%, $P < 0.0001$) and significantly lower serum levels of interleukin-10 (IL-10) than patients with MRSA bacteremia without *DNMT3A* mutation (A/C: 9.7038 pg/mL vs. A/A: 52.9898 pg/mL; $P = 0.0042$). Expression of *DNMT3A* was significantly suppressed in patients with *S. aureus* bacteremia and in *S. aureus*-challenged primary human macrophages. Small interfering RNA (siRNA) silencing of *DNMT3A* expression in human macrophages caused increased IL-10 response upon *S. aureus* stimulation. Treating macrophages with methylation inhibitor 5-Aza-2′-deoxycytidine resulted in increased levels of IL-10 when challenged with *S. aureus*. In the murine sepsis model, methylation inhibition increased susceptibility to *S. aureus*. These findings indicate that g.25498283A > C genotype within *DNMT3A* contributes to increased capacity to resolve MRSA bacteremia, potentially through a mechanism involving increased methylation of gene-regulatory regions and reduced levels of antiinflammatory cytokine IL-10.

Staphylococcus aureus | MRSA | persistence | host genetics | DNMT3A

Persistent methicillin-resistant *Staphylococcus aureus* (MRSA) bacteremia in patients despite appropriate antibiotic therapy is common, incompletely understood, and associated with poor clinical outcome (1–3). A growing body of evidence indicates that genetic variation may influence patient risk for *S. aureus* infection (4–7). In this investigation, we used a comprehensive approach to identify potential host genetic determinants of persistent methicillin-resistant *S. aureus* bacteremia (PB) and resolving methicillin-resistant *S. aureus* bacteremia (RB) in a large cohort of patients with *S. aureus* bacteremia (SAB). First, patients with PB and RB were matched on important clinical variables to minimize potential confounding factors. Second, we used whole-exome sequencing (WES) to identify candidate genetic variants associated with PB and RB. Third, we interrogated the PB and RB patient groups for differences in epigenetic phenomena, whole-blood gene expression levels, and serum cytokine levels to establish a potential pathogenic mechanism for any associations found in the WES. Fourth, we performed in vitro and in vivo experiments to support the biological plausibility of our findings.

Significance

The severity and duration of methicillin-resistant *Staphylococcus aureus* (MRSA) bacteremia varies widely between individuals. Host factors predisposing to persistent MRSA bacteremia are poorly understood, although genetic association studies are beginning to identify potentially influential variants. We found an association between the A/C heterozygous genotype in the *DNMT3A* correlating with shorter time to resolution of MRSA bacteremia. Using in vitro macrophage assays and murine sepsis models, we demonstrated that *DNMT3A* variants may alter host response to infection through increased methylation of key regulatory genes, resulting in reduced interleukin-10 production and in turn, allowing for a more protective immune response that clears infection. An improved understanding of the factors predisposing to persistent MRSA bacteremia may help to discover better treatment options.

Author contributions: F.M.M., A.S.B., S.G.F., E.F.R., D.G., M.R.Y., and V.G.F. designed research; F.M.M., B.K.S.-K., F.R., M.R., Y.-L.C., and V.G.F. performed research; B.K.S.-K., F.R., L.C.C., M.R., A.S.B., S.G.F., R.A., E.F.R., D.G., M.R.Y., and V.G.F. contributed new reagents/analytic tools; F.M.M., B.K.S.-K., F.R., M.R., Y.-L.C., L.P.P., R.A., V.G.F., and M.S.I.G. analyzed data; and F.M.M., B.K.S.-K., M.R.Y., V.G.F., and M.S.I.G. wrote the paper.

Conflict of interest statement: V.G.F. reports grant/research support from MedImmune, Cerexa/Forest/Actavis/Allergan, Pfizer, Advanced Liquid Logics, Theravance, Novartis, Cubist/Merck, Medical Biosurfaces, Locus, Affinergy, Contrafect, Karius, Genentech, Regeneron, and Basilea; is a paid consultant for Pfizer, Novartis, Galderma, Novadigm, Durata, Debiopharm, Genentech, Achaogen, Affinium, Medicines Co., Cerexa, Tetraphase, Trius, MedImmune, Bayer, Theravance, Cubist, Basilea, Affinergy, Janssen, xBiotech, Contrafect, Regeneron, Basilea, and Destiny; has membership with Merck Co-Chair V710 Vaccine; receives educational fees from Green Cross, Cubist, Cerexa, Durata, Theravance, and Debiopharm; and received royalties from UpToDate. M.R.Y. is a founder and shareholder of NovaDigm Therapeutics, Inc., which develops vaccines and immunotherapeutics targeting multidrug-resistant pathogens, including *Staphylococcus aureus*.

This article is a PNAS Direct Submission.

Data deposition: The sequence data reported in this paper have been deposited into Sequence Read Archive (SRA): https://www.ncbi.nlm.nih.gov/bioproject/PRJNA554387.

[1]D.G., M.R.Y., and V.G.F. contributed equally to this work.

[2]To whom correspondence may be addressed. Email: Vance.Fowler@duke.edu.

[3]A complete list of the MRSA Systems Immunobiology Group can be found in *SI Appendix*.

This article contains supporting information online at www.pnas.org/lookup/suppl/doi:10.1073/pnas.1909849116/-/DCSupplemental.

First published September 16, 2019.

Results

Clinical Cohort. A total of 68 patients with PB or RB were matched 1:1 by sex, age (in deciles), race, hemodialysis status, diabetes mellitus, and presence of implantable medical device (Table 1).

One Polymorphism in *DNMT3A* Differentiates between Persistent and Resolving MRSA Bacteremia. To test whether host genetic variation is associated with development of the PB phenotype, WES was performed on the 68 study patients (8). The most significantly associated variant was a single-nucleotide polymorphism (SNP), g.25498283A > C, which is located in the *DNMT3A* intronic region of chromosome 2p. The SNP was more common in RB (21 of 34, 61.8%) than PB (3 of 34, 8.8%) with a P value of 7.8×10^{-6}, which is just above a Bonferroni-corrected genome-wide level of significance (1.2×10^{-7}) (Fig. 1 and *SI Appendix*, Table S1). The g.25498283A > C mutation overlaps with open chromatin regions and known transcription factors (SP1 and EGR1) binding sites (9), suggesting that the variant might be located within a regulatory region of *DNMT3A*. Given the role of *DNMT3A* in host immune response (10) and the fact that demographic characteristics of patients with and without the SNP were similar (*SI Appendix*, Table S2), we further pursued 2 lines of investigation: 1) the potential involvement of *DNMT3A* in host response to *S. aureus* infection and 2) the potential role of variation within *DNMT3A* in patients with PB vs. RB.

***DNMT3A* Is Involved in Host Response to *S. aureus* Infection.** To evaluate the clinical relevance of *DNMT3A* in host response to *S. aureus*, we first compared the impact of *S. aureus* infection on *DNMT3A* expression using existing whole-blood microarray expression data from our previously published cohort of patients with SAB ($n = 32$) or *Escherichia coli* ($n = 19$) bacteremia (11). Relative to healthy controls, *DNMT3A* expression was significantly suppressed in patients with SAB but not *E. coli* bacteremia (Fig. 2*A*). Transcription of *DNMT3A* was also suppressed when we challenged primary human macrophages with *S. aureus* in vitro (Fig. 2*B*). Using publicly available Gene Expression Omnibus (GEO) datasets, *DNMT3A* transcription was suppressed at all tested time points in *S. aureus*-challenged human macrophages (12) (Fig. 2*C*) and at 2 and 3 h postinfection in *S. aureus*-challenged human neutrophils (13) (Fig. 2*D*). These data collectively suggest a potential role of *DNMT3A* in promoting protective immune responses to *S. aureus* infection and potential *S. aureus*-mediated dysregulation of such responses.

Patients with g.25498283A > C Exhibit Higher Methylation Levels in Gene Regulatory CpG Island Regions. We next tested whether DNA methylation patterns differed between patients with and without the g.25498283A > C mutation using reduced representation bisulfite sequencing (RRBS). The DNA methylation profile exhibited a bimodal distribution. To study the global methylation pattern at the population level, we investigated the average methylation level of each CpG region within patients with and without g.25498283A > C mutation. Study patients with the g.25498283A > C genotype exhibited significantly higher levels of methylation in gene-regulatory CpG island regions than patients with the homozygote genotype (Δmethylation = 4.1%, $P < 0.0001$) (Fig. 3). These results suggest that a global methylation increase at gene-regulatory regions is associated with the observed g.25498283A > C mutation in *DNMT3A,* and introduce a potential mechanism by which this mutation could influence host ability to resolve MRSA bacteremia.

***DNMT3A* Expression Levels Were Similar in Patients with and without g.25498283A > C.** Next, we performed whole-blood gene expression analysis to consider whether the *DNMT3A* genotype influenced expression levels. No significant differences in *DNMT3A* expression were noted between patients with ($n = 24$) or without ($n = 44$) g.25498283A > C mutation (*SI Appendix*, Fig. S1*A*). However, as the SNP of interest occurs within a noncoding region, it is possible that the mode of action occurs via a change in expression or activity of a regulatory RNA species. To test this possibility, we interrogated RNA sequencing (RNA-seq) data for the expression of regulatory RNA species. We found 2 RNA segments that were known to influence the *DNMT3A* promoter: *NUP153*, which has been shown to bind outside of the catalytic domain of *DNMT3A* with no effect in the *DNMT3A* activity, and *CDH1* (*E-cadherin*), which binds to the catalytic domain and inhibits DNMT3A activity (14). When we compared the expression levels for *NUP153* and *CDH1* between the patients with and without the polymorphism of interest, we found no significant differences between the 2 populations. Collectively, these findings suggest that the mechanism by which the DNMT3A polymorphism contributes to resolving MRSA bacteremia is not due to differences in regulatory RNA species, although the number of samples available for this analysis was limited (A/A, $n = 1$; A/C, $n = 2$) (*SI Appendix*, Fig. S1 *B* and *C*)

Patients with g.25498283A > C Exhibit Lower Levels of Interleukin-10 than Patients without the SNP. The Th2 antiinflammatory cytokine interleukin-10 (IL-10) has been previously shown to be significantly elevated in patients with poor clinical outcome among SAB patients, including mortality (15, 16), endovascular infection (17), and PB (15), and was also significantly higher in PB patients in our study (PB: 114.7472 pg/mL vs. RB: 13.1849 pg/mL; $P = 0.0009$).* Thus, we hypothesized that patients heterozygous for *DNMT3A* g.25498283A > C, who were significantly less likely to exhibit PB, would also have significantly lower levels of IL-10. To test this hypothesis, we measured IL-10 levels in acute-phase serum from the study patients using a Luminex-based 38-plex cytokine assay (*SI Appendix*, Fig. S2). Consistent with our hypothesis, patients who were A/C heterozygotes had significantly lower serum levels of IL-10 (A/C: 9.70 pg/mL vs. A/A: 52.99 pg/mL; $P = 0.0042$) than A/A patients without the *DNMT3A* mutation (Fig. 4). This pattern of lower IL-10 among heterozygotes occurred among both patients with PB (A/C: 16.88 pg/mL vs. A/A: 68.94 pg/mL) and patients with RB (A/C: 8.68 pg/mL vs. A/A: 14.95 pg/mL), although the small number of A/C patients who developed PB ($n = 3$) limited statistical comparisons. These findings suggest our working model in which patients with the A/C heterozygote genotype of *DNMT3A* were more likely to resolve MRSA bacteremia in part due to lower levels of IL-10 regulated through higher levels of methylation in gene-regulatory regions (Fig. 5).

Small Interfering RNA Knockdown of *DNMT3A* Increases IL-10 Production in Human Macrophages. We next sought to assemble biological evidence to support the plausibility of this working model. To further define the role of *DNMT3A* in regulation of the macrophage response to *S. aureus* infection, cells were treated with small interfering RNA (siRNA) specific to *DNMT3A*. Successful knockdown of *DNMT3A* was confirmed by qRT-PCR (*SI Appendix*, Fig. S3). Macrophages were then stimulated with *S. aureus*, and a Luminex-based 10-plex cytokine assay was used to evaluate the impact of *DNMT3A* knockdown on the macrophage inflammatory response to *S. aureus*. Although the expression of several cytokines was affected, only IL-10 levels were significantly altered among *S. aureus*-challenged human macrophages with siRNA-mediated knockdown of *DNMT3A* (siRNA knockdown: 232.63 pg/mL vs. scramble: 98.40 pg/mL; $P = 0.0209$) (Fig. 6*A* and *SI Appendix*, Fig. S4*A*).

*M. Rossetti *et al.*, "Early cytokine signatures discriminate persistent from resolving MRSA bacteremia" in *Federation of Clinical Immunology Societies (FOCIS) Annual Meeting* (FOCIS, Menomonee Falls, WI, 2018), Abstract W.104.

Table 1. Characteristics of patients with persistent and resolving MRSA bacteremia

	PB, $n = 34$	RB, $n = 34$	Fisher P value
Characteristic			
Age, median (P25, P75)	63 (55, 69)	61.5 (53, 70)	0.9462
Sex, no.(%)			1.00000
Male	23 (67.6)	23 (67.6)	
Female	11 (32.4)	11 (32.4)	
Race, no. (%)			1.00000
White	18 (52.9)	17 (50)	
African American	16 (47.1)	16 (47.1)	
Unknown	0 (0.0)	1(2.9)	
Underlying comorbidity, no. (%)			
Neoplasm	0 (0.0)	11 (32.4)	0.00037
Diabetic	17 (50)	20 (58.8)	0.62666
Hemodialysis dependent	13 (38.2)	9 (26.5)	0.43722
HIV positive	2 (5.9)	0 (0.0)	0.49254
Transplant recipient	1 (2.9)	6 (17.6)	0.10543
Injection drug use	1 (2.9)	0 (0.0)	1.00000
Corticosteroid use (30 d)	8 (23.5)	9 (26.5)	1.00000
Surgery past 30 d	7 (20.6)	9 (26.5)	0.77568
Endocarditis, previous episode	1 (2.9)	1 (2.9)	1.00000
Site of acquisition, no. (%)			0.52113
Hospital acquired	2 (5.9)	5 (14.7)	
HCA community acquired	30 (88.2)	26 (76.5)	
Non-HCA community acquired	2 (5.9)	3 (8.8)	
Source of bacteremia, no.(%)			0.20791
Endovascular infection	12 (35.3)	6 (17.6)	
GI/GU infection	4 (11.8)	8 (23.5)	
Respiratory/lung	2 (5.9)	1 (2.9)	
Skin, soft tissue, joint/bone infection	12 (35.3)	10 (29.4)	
None/unknown	4 (11.8)	9 (26.5)	
Other			
Metastatic infection, no. (%)	25 (73.5)	14 (41.2)	0.01356
Metastatic abscess	6 (18.2)	3 (8.8)	0.30467
Metastatic arthritis	5 (15.2)	1 (2.9)	0.10543
Metastatic epidural abscess	3 (9.1)	1 (2.9)	0.35591
Metastatic vertebral osteomyelitis	5 (15.2)	1 (2.9)	0.10543
Metastatic nonvertebral osteomyelitis	5 (15.2)	3 (8.8)	0.47628
Metastatic psoas abscess	3 (9.1)	2 (5.9)	0.67284
Metastatic septic emboli	5 (15.2)	1 (2.9)	0.10543
Metastatic septic thrombophlebitis	1 (3)	1 (2.9)	1.00000
Metastatic kidney abscess	0 (0.0)	2 (5.9)	0.49254
Metastatic endocarditis	10 (30.3)	3 (8.8)	0.03331
APACHE II, mean (SD)	18.3 (7.7)	15.8 (4.5)	
LOS categories, d, no. (%)			0.00010
<9	0 (0.0)	13 (38.2)	
9–14	9 (26.5)	10 (29.4)	
15–20	13 (38.2)	5 (14.7)	
>20	12 (35.3)	6 (17.6)	
Type of procedures used to treat the infection, no. (%)			
Surgical removal of foreign device	21 (67.7)	9 (40.9)	0.09057
Surgical debridement	11 (35.5)	2 (9.1)	0.04965
Surgical insertion of foreign device	4 (12.9)	3 (13.6)	1.00000
Abscess drainage	6 (19.4)	5 (22.7)	1.00000
Other	15 (48.4)	17 (77.3)	0.04752
Outcome (90 d), no. (%)			0.08432
Cure	27 (79.4)	33 (97.1)	
Recurrent SAB infection	4 (11.8)	1 (2.9)	
Death due to SAB infection	3 (8.8)	0 (0.0)	
Death due to other causes	0 (0.0)	0 (0.0)	

For metastatic infection, some patients have more than 1 type of metastatic infection. Some patients have more than 1 type of procedure used to treat the infection. APACHE II, Acute Physiology and Chronic Health Evaluation II; GI/GU, gastrointestinal/genitourinary; HCA, health care associated; LOS, length of stay; P, percentile.

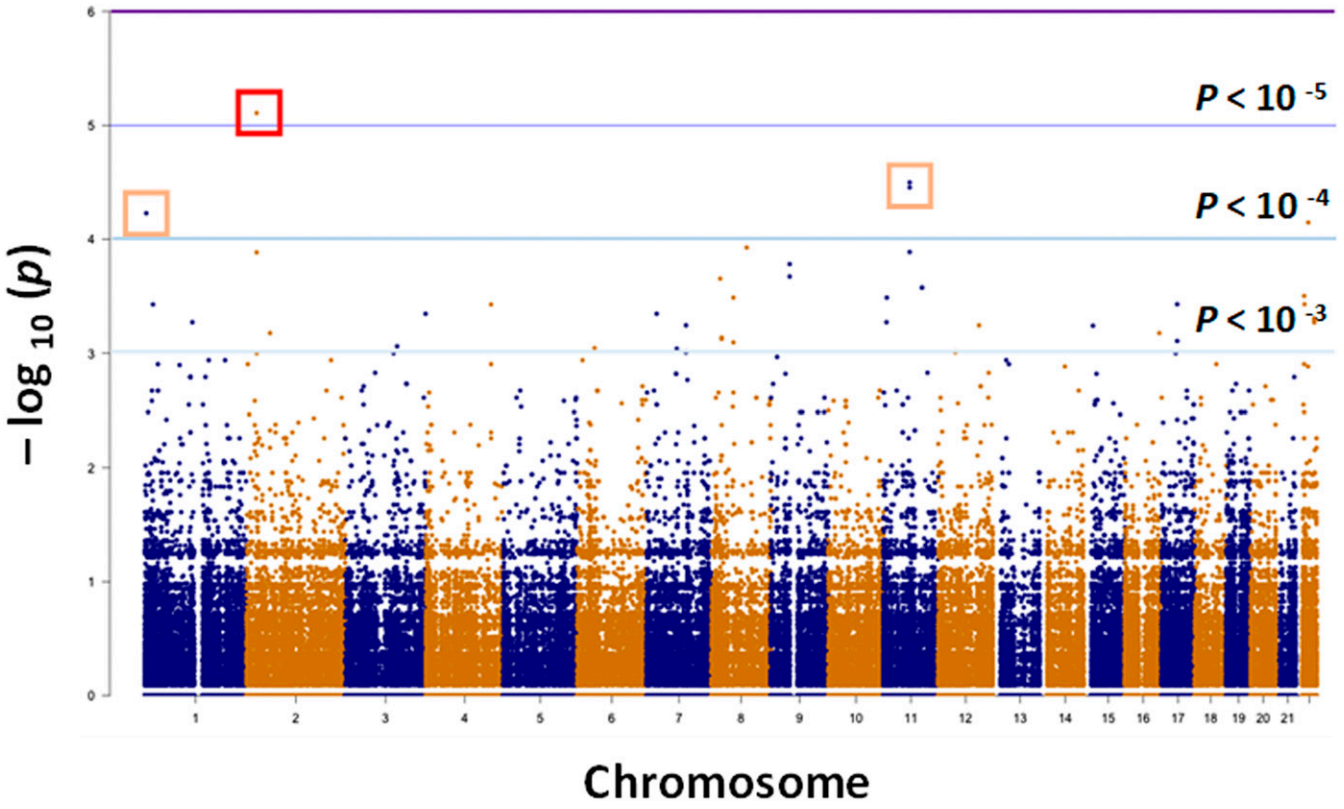

Fig. 1. Polymorphism in *DNMT3A* is associated with persistent MRSA bacteremia. The Manhattan plot of the *P* values from all SNPs. The *x* axis shows the chromosome numbers, and the *y* axis is the $-\log_{10}$ (*P* value). One SNP, g.25498283A > C in *DNMT3A*, was our most significant variant (red box). The top 20 variants (to $P < 10^{-3}$) are provided in *SI Appendix*, Table S1.

Inhibition of DNA Methylation Also Increases IL-10 Production in Human Macrophages. Because of the documented role of *DNMT3A* in DNA methylation (18) and our finding that A/C heterozygotes had higher methylation levels, we next evaluated the role of DNA methylation on human macrophage cytokine response to *S. aureus*. To do this, human macrophage methylation was inhibited by pretreatment with 5-Aza-2′-deoxycytidine (DAC), a drug known to inhibit DNA methyltransferase (19). Consistent with the increases in IL-10 production elicited by *S. aureus* challenge of human macrophages with siRNA knockdown of *DNMT3A*, inhibiting the methylation capacity of human macrophages also caused significant increases in IL-10 production after *S. aureus* challenge (DAC treatment: 353.19 pg/mL vs. phosphate-buffered saline (PBS) treatment: 235.62 pg/mL; $P = 0.0209$) (Fig. 6*B* and *SI Appendix*, Fig. S4*B*). These data agree with our working model (Fig. 5) and further support a role of *DNMT3A* in regulating cytokine production, possibly mediated by changes in DNA methylation.

Methylation Inhibition in Mice Confers Susceptibility to *S. aureus* Infection. To further elucidate the importance of *DNMT3A*-mediated methylation in host response to *S. aureus*, we inhibited methylation capacity in mice by pretreatment with DAC followed by infection with *S. aureus*. DAC-treated mice exhibited significantly greater mortality than PBS-treated controls following challenge with either methicillin-susceptible *S. aureus* (Fig. 7*A*) or MRSA (Fig. 7*B*). Bacterial load was significantly higher in the kidney, spleen, liver, and lung of DAC-treated mice than infected PBS-treated controls (Fig. 7*C*). DAC-treated mice also exhibited higher serum concentration of cytokines/chemokines than PBS-treated controls overall, although none of these differences achieved the level of statistical significance (*SI Appendix*, Fig. S5). These results suggest that methylation capacity is vital in mice to control *S. aureus* infection.

MRSA Isolates from Patients with PB and RB Elicit Similar Cytokine Response from Primary Human Macrophages but Different Levels of Macrophage Uptake. To test whether the associations between *DNMT3A* polymorphisms and the PB clinical phenotype might be specific to the infecting bacterial isolates rather than host response, we challenged primary human macrophages with representative PB or RB isolates ($n = 5$ of each) and assessed uptake and the elicited cytokine response using a 25-plex Luminex array. PB isolates exhibited significantly reduced median levels of phagocytosis by primary human macrophages compared with RB isolates (45,111.11 vs. 66,666.67 colony-forming unit [cfu]/mL; $P = 0.0292$) (Fig. 8). When we conducted the experiment with extended incubation to 24 h, RB isolates were again isolated in higher numbers from macrophages than PB isolates, although the difference did not achieve statistical significance (*SI Appendix*, Fig. S6). In the 25-plex Luminex array, only IL-8 production differed significantly in primary human macrophages challenged by PB isolates vs. RB isolates (12,610.6 vs. 14,764.4 pg/mL; $P = 0.0008$) (*SI Appendix*, Fig. S7).

Discussion

This study demonstrates that a specific polymorphism in *DNMT3A* is associated with a reduced risk for persistent MRSA bacteremia in patients, potentially through reducing IL-10 response by way of enhanced methylation. These conclusions are based on the following experimental evidence. First, g.25498283A > C in *DNMT3A* was associated with the RB phenotype at a level of significance of $P = 7.8 \times 10^{-6}$. Second, *DNMT3A* expression was suppressed by *S. aureus* in both primary human macrophages challenged with

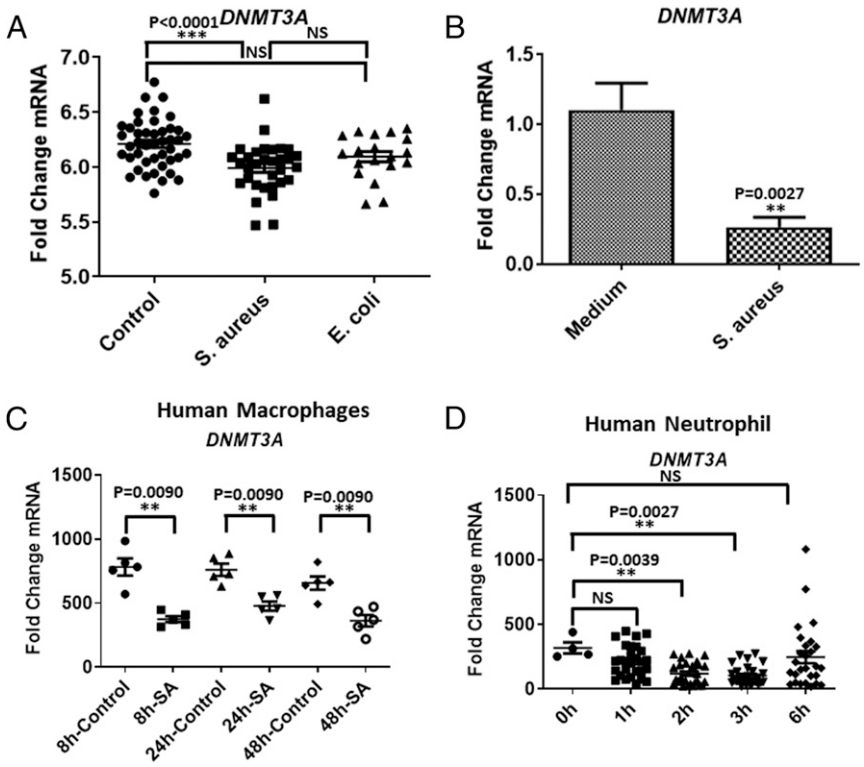

Fig. 2. *DNMT3A* transcription is suppressed by *S. aureus*. (*A*) Expression pattern of *DNMT3A* between patients with SAB, *E. coli* bacteremia, and uninfected control subjects. Human blood RNA from patients in each group was extracted and subjected to microarray. NS: not significant. (*B*) Macrophages were challenged with *S. aureus* at a multiplicity of infection of 10 for 5 h. Total RNA was extracted, and the expression of *DNMT3A* was determined by real-time PCR and normalized to that of *Actin*. Data are presented as the average and SD of points from 7 biological replicates. (*C*) Human macrophages data from public dataset GEO:GSE13670 were analyzed. *DNMT3A* was suppressed by *S. aureus* at all times tested compared with uninfected control. Data are presented as the average and SD of points from 5 biological replicates. SA: *S. aureus*. (*D*) Human neutrophils data from public dataset GEO:GSE16837 were analyzed. *DNMT3A* was suppressed by *S. aureus* at 2 and 3 h compared with 0-h control. For 0-h control, $n = 4$, and for 2 and 3 h, $n = 27$. Significance was determined using the Mann–Whitney *U* test. $^{**}P < 0.01$; $^{***}P < 0.001$.

S. aureus and patients with SAB. Third, IL-10 levels were significantly higher in patients with PB and among patients without the g.25498283A > C SNP in *DNMT3A*. Fourth, inhibition of both *DNMT3A* transcription and methylation activity led to increased IL-10 production by human macrophages upon *S. aureus* stimulation. Fifth, overall DNA methylation in patients with the g.25498283A > C mutation in *DNMT3A* was increased within gene-regulatory regions and was consistent with expectations based on our in vitro studies of *DNMT3A*. Sixth, methylation inhibition in mice rendered them significantly more susceptible to *S. aureus*. Collectively, these findings support the observation that DNA methylation is important for protective host immune defenses against *S. aureus* by way of a mechanism outlined in our working model (Fig. 5).

Although the mechanism remains incompletely understood, the observed association between g.25498283A > C mutation in *DNMT3A* and PB is consistent with previous studies. Cao et al. (20) found that a polymorphism in *DNMT3A* was associated with increased risk of *Helicobacter pylori* infection, a gram-negative bacterium responsible for gastric cancer. Other investigators have shown that mice deficient in *Dnmt3a* were susceptible to vesicular stomatitis infection (21) via impaired production of type I interferons (IFNs; IFN-α and IFN-β) (22). In T cells, *Dnmt3a* is known to regulate cytokine production with IL-13, in particular being increased in the absence of *Dnmt3a* but not *Dnmt3b* (23). These data extend insights in this regard to *S. aureus*, as IL-13 is a hallmark of Th2 immune responses that recent vaccine studies suggest do not adequately protect against *S. aureus* (24). Likewise, in mast cells, loss of *Dnmt3a* is accompanied by increased IL-13, IL-6, and tumor necrosis factor-α (TNF-α) production after stimulation with Immunoglobulin E antigen (10). However, as transforming growth factor-β (TGF-β) is required along with IL-6 and TNF-α to induce protective Th-17 polarization, change-in-function polymorphisms of *DNMT3A* could alter protective immunity against *S. aureus*. It has also been shown that mice with B cells deficient in *Dnmt3a*/*Dnmt3b* have increased cell activation when immunized with phycoerythrin emulsified in complete Freud's adjuvant (25). Consistent with the pattern of generally increased cytokine production in *DNMT3A*-deficient cells, we found that siRNA knockdown of *DNMT3A* or inhibition with DAC in human macrophages resulted in increased levels of cytokine IL-10 production upon *S. aureus* stimulation.

IL-10, an immunosuppressive cytokine produced primarily in the Th2 paradigm, has been identified as a potential marker of immune dysregulation associated with persistent SAB and/or mortality (15). IL-10 is known to block the activation of Th1 cells, thereby promoting susceptibility to certain intracellular pathogens (26, 27). One role for IL-10 is in regulation of the production of proinflammatory cytokines and has been shown to play an essential role during *S. aureus* infection: too much IL-10 expression biases toward death of the infected host (28). IL-10 has also been shown to inhibit microbial killing by limiting the production of reactive oxygen and nitrogen intermediates (29, 30). In *Mycobacterium tuberculosis* infection, IL-10 blocks phagosome maturation and facilitates *M. tuberculosis* survival (31). Transgenic mice overexpressing IL-10 in T cells are more susceptible to *M. tuberculosis* infection (32). Elevation in serum IL-10 has also been described in humans with active

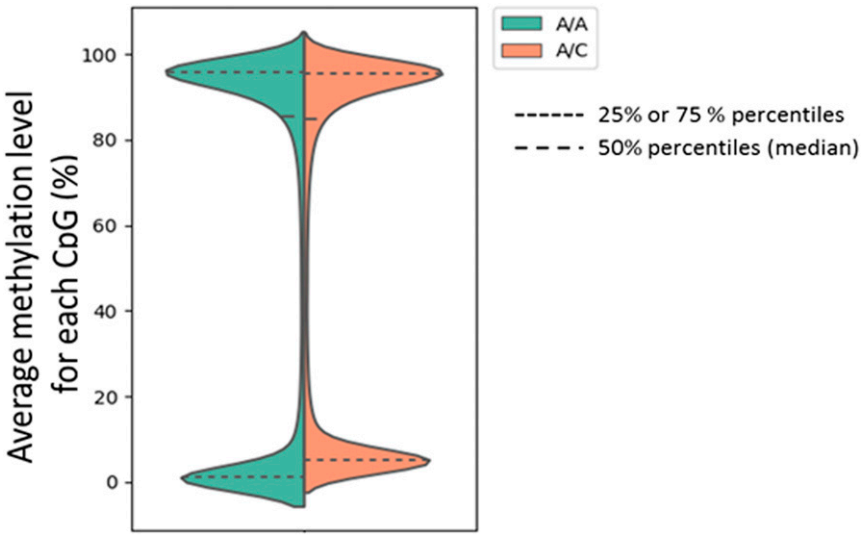

Fig. 3. Polymorphism in *DNMT3A*-dysregulated DNA methylation in patients. The DNA methylation levels in PB and RB patients were measured by RRBS. The violin plot shows the distribution of the CpG counts at each average methylation level for patients without the mutation (A/A [green]: $n = 44$) and patients with the g.25498283A > C mutation (A/C [salmon]: $n = 24$). The median test was computed to compare the differences between patients with and without g.25498283A > C mutation. Patients with the g.25498283A > C mutation exhibited significantly higher levels of methylation in gene-regulatory CpG island regions than patients with the homozygote genotype (Δmethylation = 4.1%; $P < 0.0001$).

pulmonary tuberculosis (33), thereby establishing a direct correlation between IL-10 level and disease severity.

Our study had limitations. First, the polymorphism is located in the noncoding region of *DNMT3A*. Thus, it is not possible to predict any direct effect of the polymorphism on *DNMT3A* function. Second, the mutation did not impact the transcription of *DNMT3A* messenger RNA (mRNA); therefore, the siRNA model system used in this manuscript may not accurately represent the effect of the polymorphism observed with WES. Our proof of concept study using DAC-treated mice has the potential for broader, off-target effects of DAC. Thus, additional experiments are underway in our laboratory to determine the specific association between *DNMT3A* polymorphisms and persistent *S. aureus* infection using knockout mice. Third, we recognize that certain subsets of IL-10–producing CD4+ T cells are proinflammatory (34). Thus, IL-10 should not be exclusively defined as antiinflammatory; rather, IL-10 likely functions in context of other responses that collectively shape protective vs. nonprotective immunity to a given pathogen in a specific host. Fourth, the causes of persistent MRSA bacteremia are complex. For example, we found that bacteria from patients with PB and RB interacted differently with human macrophages, eliciting different levels of phagocytosis and triggering different levels of IL-8 from these cells. Thus, it is likely that a number of clinical and bacterial characteristics in addition to the patient's DNMT3A genotype may also contribute to this clinical syndrome. Fifth, there are undoubtedly additional cytokines or other molecular and cellular immune responses not presently studied that contribute to the PB vs. RB outcome. Susceptibility to host defense peptides and binding to endothelial cells are 2 examples of MRSA phenotypes that also seem to influence PB vs. RB outcomes (35).

Despite these limitations, this study provides evidence that the g.25498283A > C polymorphism in *DNMT3A* protects against persistent MRSA bacteremia by changing patterns in DNA methylation. The findings establish epigenetic modification of DNA as influencing host response to *S. aureus* infection. Future studies are underway to elucidate the molecular mechanisms of how this polymorphism influences the risk for PB. The ability of advanced bioinformatics tools to assess global genome methylation patterns across all regions of the human genome will greatly facilitate this goal.

Material and Methods

Clinical Cohort. The *S. aureus* Bacteremia Group Prospective Cohort Study has prospectively enrolled all eligible adult, hospitalized, nonneutropenic patients with monomicrobial SAB at Duke University Medical Center since September 1994. Patients were excluded from the study if they were <18 y of age, were neutropenic (defined as an absolute neutrophil count $\leq 1 \times 10^9$/L), were not admitted to the hospital, were previously enrolled for another

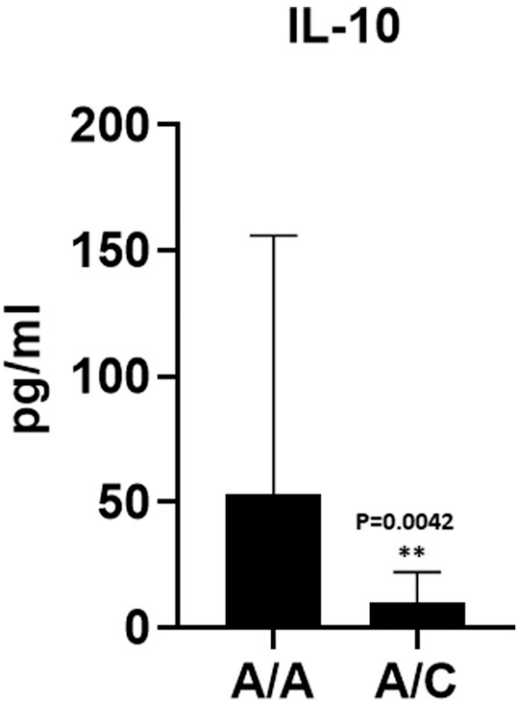

Fig. 4. Serum IL-10 concentration is lower in patients with A/C genotype than A/A. Serum cytokine production was determined using human 38-plex magnetic cytokine/chemokine kits. Before testing, IL-10 levels (picograms per milliliter) were log transformed to satisfy normality assumptions and to mitigate variance heterogeneity. $^{**}P < 0.01$ (A/C: $n = 24$ and A/A: $n = 44$).

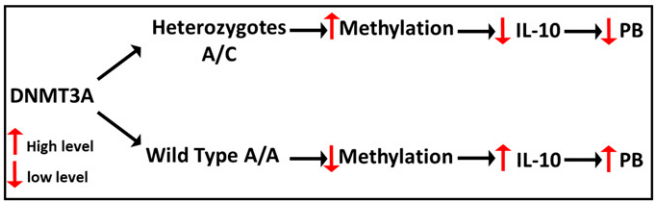

Fig. 5. Working model of *DNMT3A* polymorphism and persistent MRSA bacteremia.

SAB episode, had no signs or symptoms of infection, had an additional clinically significant bacterial pathogen that was isolated from their blood culture, or declined informed consent. Only the initial presentation for eligible patients was included in the study. Clinical data were collected on a standardized case report form and entered into an electronic database (Microsoft Access). The outcomes of SAB per study protocol recorded deaths (attributable to *S. aureus* or other causes), cure, or recurrent bacteremia within the 90-d follow-up period. The study was approved by the Duke Institutional Review Board. Written informed consent was obtained from patients or their legal representatives. If a patient died prior to the notification of their blood culture results, the subjects were included using an Institutional Review Board-approved Notification of Decedent Research.

Patients were defined as having either PB or RB. PB patients ($n = 34$) had ongoing MRSA bacteremia for at least 5 d after initiation of effective antibiotics. Patients with RB had initial blood cultures that were positive for MRSA, but all subsequent blood cultures were sterile. PB and RB patients were eligible for inclusion if all required biological samples were available (sera/plasma, RNA, DNA, and bloodstream isolate), and they were successfully matched 1:1 by sex, age (by deciles), race, hemodialysis status, diabetes mellitus, and presence of any implantable medical device using nearest neighbor propensity scores (36) generated from logit regression models fit separately across 4 strata.

WES and Analysis. DNA-Seq data were processed using the TrimGalore toolkit (37) (v0.4.0), which uses Cutadapt (v1.8.3) to trim low-quality bases and Illumina sequencing adapters from the 3′ end of the reads. Reads were aligned to the b37 version of the human genome with the BWA algorithm (v0.7.12). Alignment processing and variant calling were performed using the GATK toolkit (v3.7) following the Broad Institute's Best Practices Workflow (38). Association testing was carried out using the Fisher's exact test from the RVTESTS algorithm (39) (v20150104).

RNA-seq in PB and RB Patients. Total RNA was isolated with the Qiagen RNA Blood kit, and quality control was performed with Nanodrop 8000 and Agilent Bioanalyzer 2100. Globin RNA was removed with the Life Technologies GLOBINCLEAR (human) kit. Libraries for RNA-seq were prepared with the KAPA Stranded mRNA-Seq Kit. The workflow consists of mRNA enrichment, complementary DNA (cDNA) generation, and end repair to generate blunt ends, A tailing, adaptor ligation, and PCR amplification. Different adaptors were used for multiplexing samples in 1 lane. Sequencing was performed on an Illumina Hiseq3000 for a single-read 50 run. Each sample gets an average of 15 million reads. Data quality check was done on Illumina SAV. Demultiplexing was performed with the Illumina Bcl2fastq2 v 2.17 program.

DNA Methylation Levels in A/A and A/C Patients. The DNA methylation levels in patients with and without the g.25498283A > C mutation were measured by RRBS as previously described (40). The detectable CpGs were determined based on the filter of 15× coverage. The average methylation level for each CpG in patients with or without g.25498283A > C mutation was calculated using python package scipy. The violin plot demonstrated the distributions of the CpG counts at each averaged methylation level generated by python library seaborn. The median test was computed to compare the differences between patients with and without g.25498283A > C mutation in STATA.

Serum/Plasma 38-Plex Cytokine/Chemokine Array. Luminex assay and analysis were performed by the University of California, Los Angeles Immune Assessment Core. Human 38-plex magnetic cytokine/chemokine kits (EMD Millipore; HCYTMAG-60K-PX38) were used per the manufacturer's instructions. Fluorescence was quantified using a Luminex 200 instrument. Cytokine/chemokine concentrations were calculated using Milliplex Analyst software version 4.2 (EMD Millipore).

Measurement of Cytokines in In Vitro Assays. Cytokine production was assayed from the supernatant of either *S. aureus*-challenged siRNA-transfected macrophages or *S. aureus*-challenged DAC-treated macrophages using a multiplex cytokine kit and Luminex technology available at the Duke Human Vaccine Institute. Ten cytokines were tested: TNF-α, IL-1β, IL-2, IFN-γ, IL-4, IL-5, IL-6, IL-10, IL-8, and granulocyte-macrophage colony-stimulating factor (GM-CSF). Of the 10 tested cytokines, 5 for siRNA (IL-1β, IL-5, IFN-γ, IL-2, and IL-4) and 6 for DAC (IL-1β, IL-5, IFN-γ, IL-2, IL-4, and GM-CSF) were excluded from our analysis due to lack of response to *S. aureus*; 1 cytokine GM-CSF for siRNA and 1 cytokine TNF-α for DAC were excluded for weak signal or unproven running, and 1 cytokine (IL-8 for both siRNA and DAC) was excluded for cross-contamination (*SI Appendix*, Fig. S3). For cytokines/chemokines production in human macrophages challenged with persistent and resolving isolates, 25 cytokines were tested: IL-1β, IL-10, IL-6, RANTES, Eotaxin, IL-17A, MIP-1α, GM-CSF, MIP-1β, MCP-1, IL-15, IL-5, IFN-γ, IFN-α, IL-1RA, TNF-α, IL-2, IL-7, IP-10, IL-2R, MIG, IL-4, IL-8, IL-12, and IL-13. Of those, 9 (IL-1β, RANTES, Eotaxin, IL-17A, GM-CSF, IL-5, IL-2, IL-7, and IL-13) were excluded from our analysis due to lack of response to *S. aureus*; 2 (IP-10 and IFN-γ) were excluded for weak signal, and 3 (IL-1RA, IFN-α, and MCP-1) were excluded cross-contamination.

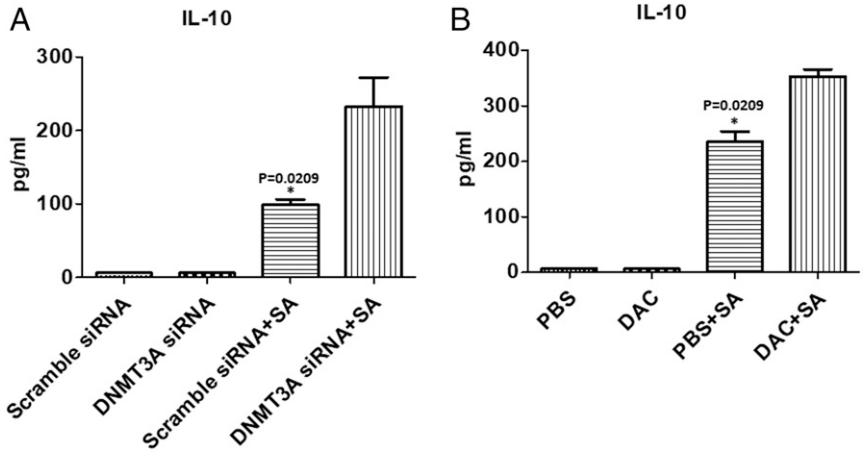

Fig. 6. (*A*) siRNA knockdown or (*B*) DAC treatment of human macrophages increases IL-10 production. Primary human macrophages were treated with either *DNMT3A* siRNA or DAC, then incubated with *S. aureus* at a multiplicity of infection of 10 for 5 h, after which macrophage culture supernatants were collected for cytokine analysis. The IL-10 profile was determined by Luminex-based multiplex cytokine assay. Data are presented as the average and SD of points from 4 biological replicates. Significance was determined using the Mann–Whitney *U* test. *$P < 0.05$.

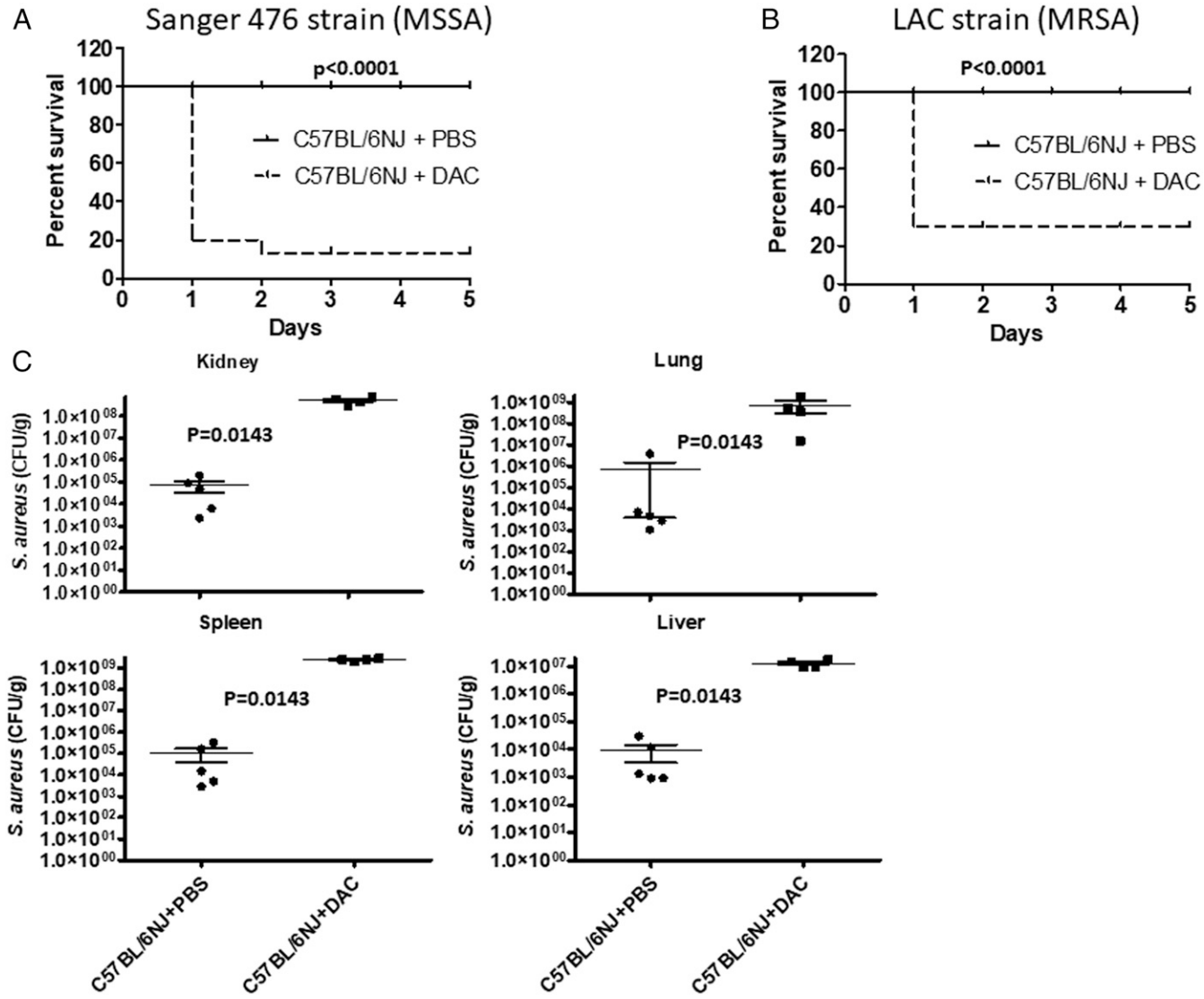

Fig. 7. Mice treated with DAC are hypersusceptible to *S. aureus* with high bacterial tissue burden. (*A*) Survival curve of 8-wk-old C57BL/6NJ-DAC and C57BL/6NJ-PBS mice after intraperitoneal injection of 10^8 cfu of methicillin-susceptible *S. aureus* (MSSA) strain Sanger 476 per mouse ($n = 15$ per group). (*B*) Survival curve of 8-wk-old C57BL/6NJ-DAC and C57BL/6NJ-PBS mice after intraperitoneal injection of 4×10^7 cfu of methicillin-resistant *S. aureus* (MRSA) LAC strain per mouse (C57BL/6NJ-DAC, $n = 10$; C57BL/6NJ-PBS, $n = 9$). Survival analysis was done using the log rank test ($P < 0.001$). (*C*) Increased bacterial load in DAC-treated and PBS-treated mice after *S. aureus* infection. DAC-treated and PBS-treated controls were injected intraperitoneally with *S. aureus* strain Sanger 476, and the bacterial loads in kidneys, spleens, livers, and lungs were determined 18 h postinfection. Significant difference in bacterial load between DAC-treated and PBS-treated control mice was done using the Mann–Whitney *U* test ($P < 0.05$). At least 4 mice per group were analyzed.

Bacterial Strains and Growth Conditions. Sanger 476, a methicillin-susceptible *S. aureus* (41), and LAC, an MRSA isolate (42), were used in this study. *S. aureus* was prepared as previously described (43) with minor modifications. After overnight culture, an appropriate number of cells were diluted to 500 mL fresh tryptic soy broth to achieve an optical density at wavelength 600 nm (OD 600) of 0.1. The flasks were incubated at 37 °C and 220 rpm to log-phase growth (OD 600 ~ 1.0). Cells were harvested by centrifugation, washed twice with PBS, resuspended in PBS containing 20% glycerol to a concentration of ~10^6 cfu/μL, aliquoted into individual cryovials, and immediately stored at −80 °C until further use. An aliquot of PBS-washed culture was serially diluted and plated on Trypticase soy agar plates to enumerate cfu. Frozen stocks were titered for cfu in triplicate on separate occasions before use in any experiment.

Mammalian Cell Culture. Primary human macrophages were derived from peripheral blood monocytes isolated from whole blood taken from healthy volunteers (Nebraska Medical School). Monocytes were cultured in Dulbecco's Modified Eagle's Medium containing 10% (vol/vol) true pooled human serum (serocase) supplemented with 0.1% gentamycin (Sigma) and recombinant human macrophage colony-stimulating factor (M-CSF) at 6 ng/mL (RD systems). After 3 d of culture, fresh medium was added to dilute out M-CSF and antibiotic, and every other day, half of the medium was replaced with fresh medium for up to 7 d, at which point cells were ready for functional study.

siRNA Transfection. Differentiated primary human macrophages were transfected with either siRNA targeting *DNMT3A* or control scramble siRNA (Dharmacon). Stocks of siRNA along with the scramble siRNA were diluted to 10 μM with RNase free water. Prior to transfection, siRNAs were added to Opti-MEM (Thermo Fisher Scientific); then, the solution was combined with lipofectamine RNAiMAX (Thermo Fisher Scientific) and incubated at room temperature for 10 min for complex formation. After the siRNAs complex was added to the cells to a final concentration of 50 nM and cells were incubated in a 37 °C and 5% CO_2 incubator for 24 h, the cells were washed with PBS and then, challenged with *S. aureus*. The efficiency of *DNMT3A* knockdown was measured by qRT-PCR.

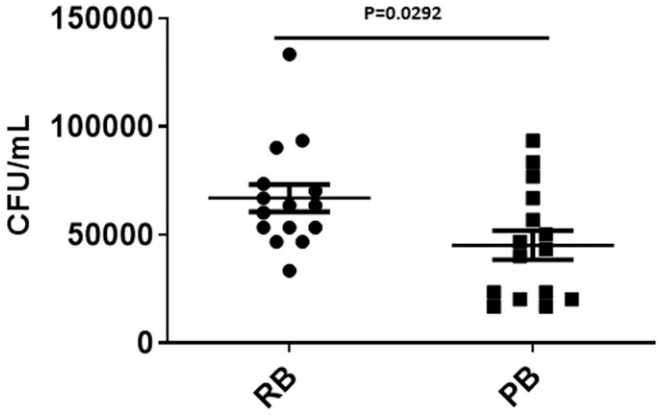

Fig. 8. MRSA bloodstream isolates from patients with persistent and resolving bacteremia elicit different phagocytosis by primary human macrophages. Differentiated macrophages were incubated with *S. aureus* isolates for 30 min; following infection, cells were treated with gentamicin (100 μg/mL) for 2 h. After treatment, cells were washed and lysed, and the resulting intracellular bacteria were plated for cfu. Means and SD of 5 persistent and 5 resolving isolates, with each including 3 biological replicates. Significance was determined using Mann–Whitney *U* test ($P < 0.05$).

DAC Treatment of Human Macrophages. Cells were seeded at a density of 5×10^5 cells per well in a 24-well plate (VWR). Dissolved DAC (Sigma) was added to cells to achieve a final concentration of 5 μM, and cells were incubated in a 37 °C and 5% CO_2 incubator for 72 h. After the treatment, the medium was replaced with fresh medium without DAC, and the cells were challenged with *S. aureus*.

RNA Extraction, cDNA Conversion, and qRT-PCR. Total RNA was extracted using the Direct-zol RNA MiniPrep kit (Zymo Research) and was subsequently digested with DNase I (Zymo Research). The concentration and purity were evaluated using the NanoDrop ND-1000 spectrophotometer (NanoDrop Technologies). RNA was reverse transcribed using the SuperScript III Reverse Transcriptase Kit (Thermo Fisher). qRT-PCR was performed using a Power SYBR Select Mater Mix (Life Technologies) and an ABI Prism 7500 Fast real-time PCR system (Life Technologies). All kits were used according to the manufacturer's instructions. The mRNA of *DNMT3A* was normalized to *Actin* ribosomal RNA. The *DNMT3A* and *Actin* primers used here are as follow: DNMT3A (5′-TATTGATGAGCGCACAAGAGAGC-3′/5′-GGGTGTTCCAGGGTAACATTGAG-3′) and Actin (5′-CACCAACTGGGACGACAT-3′/5′-ACAGCCTGGATAGCAACG-3′).

In Vivo Experiment. C57BL/6NJ mice were purchased from the Jackson Laboratory and housed in a specific pathogen-free facility. The experimental protocol was approved by the Duke University Animal Care and Use Committee, and animals were handled in accordance with their guidelines. Mice were injected via an intraperitoneal route with DAC (44) at a dose of 0. 2 mg/kg in 100 μl PBS for 5 consecutive days. Controls mice were given an appropriate volume of PBS. After treatment, both groups were challenged via the intraperitoneal route with *S. aureus* strains and monitored for morbidity every 8 h for a total of 5 d.

Tissue Bacterial Culture. For tissue bacterial culture, mice were euthanized at 18 h postinjection. Tissues were isolated and weighed under sterile conditions, and they were homogenized in PBS followed by serial dilution; each dilution was plated on Tryptic Soy Agar (Becton Dickinson). Plates were incubated overnight at 37 °C; the number of colonies was counted and multiplied by the corresponding dilution factor, and the result is expressed as cfu per gram.

5-Methylcytosine Measurements. Briefly, genomic DNA (gDNA) was isolated from mice tails using a DNeasy Blood & Tissue Kit (Qiagen). The gDNA (100 ng) was coated with 5-methylcytosine (5-mC) coating buffer and then, immediately denatured at 98 °C for 5 min in a thermal cycler. The denaturing DNA was blocked with 5-mC Elisa buffer, and 5-mC levels in gDNA were determined using and anti–5-mC antibody (Zymo Research).

Statistical Analysis. Standard *t* tests were conduct via STATA (45) to compare mean IL-10 levels among mutant and wild-type *Dnmt3a* individuals. Before testing, IL-10 levels (picograms per milliliter) were log transformed to satisfy normality assumptions and to mitigate variance heterogeneity. All *P* values were 2 sided, and no adjustment for multiple comparisons was made here. (For completeness, the additional tests comparing *Dnmt3a* groups for PB and RB subgroups were formulated post hoc and are considered exploratory.)

Demographic and clinical characteristics for the persistent and resolving bacteremia patients as well as for the DNMT3A genotype groups are presented as counts and percentages for categorical variables and as medians and quartiles for the continuous measures. Statistical comparisons comparing the groups were performed with Fisher's exact test and the Mann–Whitney *U* test as appropriate. Differences in experimental results for continuous measures were also compared with the Mann–Whitney *U* test, and statistical differences in survival of experimental are displayed as Kaplan–Meier curves and tested with the log rank test. *P* values of <0.05 were considered statistically significant. These analyses were conducted with SAS 9.4 (SAS Institute).

ACKNOWLEDGMENTS. These studies were supported by NIH Grants U01-AI124319, R33-AI111611, and R01-AI068804. V.G.F. was supported by NIH Grant K24-AI093969.

1. V. G. Fowler Jr *et al*., Clinical identifiers of complicated *Staphylococcus aureus* bacteremia. *Arch. Intern. Med.* **163**, 2066–2072 (2003).
2. C. Hawkins *et al*., Persistent *Staphylococcus aureus* bacteremia: An analysis of risk factors and outcomes. *Arch. Intern. Med.* **167**, 1861–1867 (2007).
3. J. R. Johnson, Persistent *Staphylococcus aureus* bacteremia. *Arch. Intern. Med.* **168**, 772–773 (2008).
4. D. D. Cyr *et al*., Evaluating genetic susceptibility to *Staphylococcus aureus* bacteremia in African Americans using admixture mapping. *Genes Immun.* **18**, 95–99 (2017).
5. G. N. DeLorenze *et al*., Polymorphisms in HLA class II genes are associated with susceptibility to *Staphylococcus aureus* infection in a white population. *J. Infect. Dis.* **213**, 816–823 (2016).
6. J. A. Messina, J. T. Thaden, B. K. Sharma-Kuinkel, V. G. Fowler Jr, Impact of bacterial and human genetic variation on *Staphylococcus aureus* infections. *PLoS Pathog.* **12**, e1005330 (2016).
7. W. K. Scott *et al*., Human genetic variation in *GLS2* is associated with development of complicated *Staphylococcus aureus* bacteremia. *PLoS Genet.* **14**, e1007667 (2018).
8. F. Mba Medie *et al*., Genetic variation of DNA methyltransferase-3A contributes to protection against persistent MRSA bacteremia in patients. Sequence Read Archive. https://www.ncbi.nlm.nih.gov/bioproject/PRJNA554387. Deposited 13 July 2019.
9. L. Ho, G. R. Crabtree, Chromatin remodelling during development. *Nature* **463**, 474–484 (2010).
10. C. Leoni *et al*., *Dnmt3a* restrains mast cell inflammatory responses. *Proc. Natl. Acad. Sci. U.S.A.* **114**, E1490–E1499 (2017).
11. S. H. Ahn *et al*., Gene expression-based classifiers identify *Staphylococcus aureus* infection in mice and humans. *PLoS One* **8**, e48979 (2013).
12. J. Koziel *et al*., Data from "Gene expression data from *S. aureus*-exposed macrophages." Figshare. https://www.ncbi.nlm.nih.gov/geo/query/acc.cgi?acc=GSE13670. Deposited 19 November 2008.
13. A. M. Palazzolo-Ballance *et al*., Data from "Gene expression data from *S. aureus*-exposed neutrophils." Figshare. https://www.ncbi.nlm.nih.gov/geo/query/acc.cgi?acc=GSE16837. Deposited 25 June 2009.
14. C. Holz-Schietinger, N. O. Reich, RNA modulation of the human DNA methyltransferase 3A. *Nucleic Acids Res.* **40**, 8550–8557 (2012).
15. A. O. Guimaraes *et al*., A prognostic model of persistent bacteremia and mortality in complicated *Staphylococcus aureus* bloodstream infection. *Clin. Infect. Dis.* **68**, 1502–1511 (2019).
16. W. E. Rose *et al*., Elevated serum interleukin-10 at time of hospital admission is predictive of mortality in patients with *Staphylococcus aureus* bacteremia. *J. Infect. Dis.* **206**, 1604–1611 (2012).
17. W. E. Rose *et al*., Increased endovascular *Staphylococcus aureus* inoculum is the link between elevated serum interleukin 10 concentrations and mortality in patients with bacteremia. *Clin. Infect. Dis.* **64**, 1406–1412 (2017).
18. Z. M. Zhang *et al*., Structural basis for DNMT3A-mediated de novo DNA methylation. *Nature* **554**, 387–391 (2018).
19. J. K. Christman, 5-Azacytidine and 5-aza-2′-deoxycytidine as inhibitors of DNA methylation: Mechanistic studies and their implications for cancer therapy. *Oncogene* **21**, 5483–5495 (2002).
20. X. Y. Cao *et al*., DNMT3a rs1550117 polymorphism association with increased risk of Helicobacter pylori infection. *Asian Pac. J. Cancer Prev.* **14**, 5713–5718 (2013).
21. X. Li *et al*., Methyltransferase Dnmt3a upregulates HDAC9 to deacetylate the kinase TBK1 for activation of antiviral innate immunity. *Nat. Immunol.* **17**, 806–815 (2016).
22. F. McNab, K. Mayer-Barber, A. Sher, A. Wack, A. O'Garra, Type I interferons in infectious disease. *Nat. Rev. Immunol.* **15**, 87–103 (2015).
23. Q. Yu *et al*., DNA methyltransferase 3a limits the expression of interleukin-13 in T helper 2 cells and allergic airway inflammation. *Proc. Natl. Acad. Sci. U.S.A.* **109**, 541–546 (2012).
24. C. D. Dupont *et al*., Two vaccines for *Staphylococcus aureus* induce a B-cell-mediated immune response. *MSphere* **3**, e00217–e00218 (2018).

25. B. G. Barwick *et al*., B cell activation and plasma cell differentiation are inhibited by de novo DNA methylation. *Nat. Commun.* **9**, 1900 (2018).
26. D. F. Fiorentino, M. W. Bond, T. R. Mosmann, Two types of mouse T helper cell. IV. Th2 clones secrete a factor that inhibits cytokine production by Th1 clones. *J. Exp. Med.* **170**, 2081–2095 (1989).
27. P. S. Redford, P. J. Murray, A. O'Garra, The role of IL-10 in immune regulation during *M. tuberculosis* infection. *Mucosal Immunol.* **4**, 261–270 (2011).
28. J. M. Leech, K. A. Lacey, M. E. Mulcahy, E. Medina, R. M. McLoughlin, IL-10 plays opposing roles during *Staphylococcus aureus* systemic and localized infections. *J. Immunol.* **198**, 2352–2365 (2017).
29. R. T. Gazzinelli, I. P. Oswald, S. L. James, A. Sher, IL-10 inhibits parasite killing and nitrogen oxide production by IFN-gamma-activated macrophages. *J. Immunol.* **148**, 1792–1796 (1992).
30. S. Redpath, P. Ghazal, N. R. Gascoigne, Hijacking and exploitation of IL-10 by intracellular pathogens. *Trends Microbiol.* **9**, 86–92 (2001).
31. S. O'Leary, M. P. O'Sullivan, J. Keane, IL-10 blocks phagosome maturation in *mycobacterium tuberculosis*-infected human macrophages. *Am. J. Respir. Cell Mol. Biol.* **45**, 172–180 (2011).
32. L. Moreira-Teixeira *et al*., T cell-derived IL-10 impairs host resistance to *Mycobacterium tuberculosis* infection. *J. Immunol.* **199**, 613–623 (2017).
33. A. Verbon *et al*., Serum concentrations of cytokines in patients with active tuberculosis (TB) and after treatment. *Clin. Exp. Immunol.* **115**, 110–113 (1999).
34. L. Brockmann *et al*., Molecular and functional heterogeneity of IL-10-producing $CD4^+$ T cells. *Nat. Commun.* **9**, 5457 (2018).
35. K. Seidl *et al*., Combinatorial phenotypic signatures distinguish persistent from resolving methicillin-resistant *Staphylococcus aureus* bacteremia isolates. *Antimicrob. Agents Chemother.* **55**, 575–582 (2011).
36. P. R. Rosenbaum, D. B. Rubin, The central role of the propensity score in observational studies for causal effects. *Biometrika* **70**, 41–55 (1983).
37. A. Gupta, I. K. Jordan, L. Rishishwar, stringMLST: A fast k-mer based tool for multilocus sequence typing. *Bioinformatics* **33**, 119–121 (2017).
38. M. A. DePristo *et al*., A framework for variation discovery and genotyping using next-generation DNA sequencing data. *Nat. Genet.* **43**, 491–498 (2011).
39. G. A. Van der Auwera *et al*., From FastQ data to high confidence variant calls: The genome analysis toolkit best practices pipeline. *Curr. Protoc. Bioinformatics* **43**, 1–33 (2013).
40. K. Fu *et al*., A temporal transcriptome and methylome in human embryonic stem cell-derived cardiomyocytes identifies novel regulators of early cardiac development. *Epigenetics* **13**, 1013–1026 (2018).
41. S. H. Ahn *et al*., Two genes on A/J chromosome 18 are associated with susceptibility to *Staphylococcus aureus* infection by combined microarray and QTL analyses. *PLoS Pathog.* **6**, e1001088 (2010).
42. B. A. Diep *et al*., Complete genome sequence of USA300, an epidemic clone of community-acquired meticillin-resistant *Staphylococcus aureus*. *Lancet* **367**, 731–739 (2006).
43. B. K. Sharma-Kuinkel *et al*., Potential influence of *Staphylococcus aureus* clonal complex 30 genotype and transcriptome on hematogenous infections. *Open Forum Infect. Dis.* **2**, ofv093 (2015).
44. K. Kozar *et al*., Interleukin 12-based immunotherapy improves the antitumor effectiveness of a low-dose 5-Aza-2′-deoxycitidine treatment in L1210 leukemia and B16F10 melanoma models in mice. *Clin. Cancer Res.* **9**, 3124–3133 (2003).
45. StataCorp, Stata: Release 14. Statistical Software (StataCorp LLC, College Station, TX, 2015).